Carrier-mediated ferromagnetism in N codoped (Zn,Mn)O $(10\bar{1}0)$ thin films

Q. Wang, Q. Sun, and P. Jena*
Physics Department, Virginia Commonwealth University, Richmond, Virginia 23284-2000, USA

Y. Kawazoe
Institute for Material Research, Tohoku University, Sendai, 980-8577, Japan
(Received 13 May 2004; published 31 August 2004)

Using first principles calculations based on the density functional theory and generalized gradient approximation we show that the ground state of Mn doped ZnO $(10\bar{1}0)$ thin film changes from antiferromagnetic to ferromagnetic when codoped with N. The ferromagnetic coupling between Mn spins arises due to the overlap between N 2*p* and Mn 3*d* electrons in the spin up band, rendering the system half-metallic character.

DOI: 10.1103/PhysRevB.70.052408 PACS number(s): 71.55.−i, 61.72.Ss, 71.15.Nc

The potential of dilute magnetic semiconductor materials for applications in electronic and magnetic devices has created considerable interest in the study of III–V and II–VI semiconductors doped with transition metal impurities. Of these, the most extensively studied systems are (Ga,Mn)N and (Zn,Mn)O as these were predicted to be ferromagnetic at or above room temperature.[1] As a host material, ZnO has certain advantages over GaN. It is transparent and up to 35% Mn can be doped into ZnO by the pulsed laser technique.[2] This leads to the possibility that optoelectronic devices could be fabricated if transparent (Zn,Mn)O could be made into a ferromagnet at room temperature.

Considerable experimental work is available on the (Zn,Mn)O system.[3] However, the results have been rather controversial. While some groups have reported ferromagnetism in (Zn,Mn)O systems,[4,5] others report observations of antiferromagnetic or spin-glass behavior.[6] Similarly conflicting results also exist concerning the distribution of Mn in ZnO. Some authors[7] find Mn to be distributed homogeneously, yet others report clustering of Mn atoms.[8] In addition, Rao and co-workers[9] have recently shown that sample preparation conditions are critical to observing ferromagnetism in (Zn,Mn)O.

There have been several theoretical studies as well on this system. However, most of these are confined to Mn substitution in bulk ZnO crystal. Using the Korringa-Kohn-Rostoker method combined with the coherent potential approximation, Katayama-Yoshida and Sato[10] have shown that Mn doped ZnO has an antiferromagnetic ground state. These authors used a 16-atom supercell in which two Zn atoms were replaced by Mn atoms, thus leading to a Mn concentration of 25%. They used the lattice parameters as given experimentally for ZnO and no attempts were made in relaxing the geometry of the supercell after Mn substitution. Their results were based on the local density approximation to the density functional theory. A recent theoretical and experimental study, however, reports a ferromagnetic ground state for the same system with a Mn concentration of 4.2%.[5] Little attention has been given to the theoretical study of thin films synthesized under nonequilibrium conditions, such as molecular beam epitaxy, metalorganic chemical vapor deposition, and pulsed laser deposition. Under these conditions the structural relaxations can be significant. In addition, the results may also depend upon the sites Mn and other codoped atoms occupy. We have recently calculated the total energies of a (Zn,Mn)O $(10\bar{1}0)$ thin film with 12.5% Mn substituted at the Zn site. The ground state of the film was found to be antiferromagnetic with the ferromagnetic state lying 0.133 eV/Mn atom above the ground state.

In this paper we report a theoretical study of (Zn,Mn)O thin film codoped with N, and show that this codoping can change the ground state from antiferromagnetic to ferromagnetic. We have chosen the $(10\bar{1}0)$ surface of ZnO having wurtzite structure. The thin film was modeled by a slab consisting of eight layers. The top and bottom surfaces were separated from other slabs in a supercell geometry by introducing a vacuum region of 10 Å. The center four layers of this slab were fixed at the bulk crystalline position while the top two and bottom two layers of the slab were relaxed without symmetry constraint. The supercell consists of 32 Zn and 32 O atoms as shown in Fig. 1. To study the effect of Mn and N codoping on the properties of ZnO, we have replaced Zn sites with Mn and O sites with N in the $Zn_{32}O_{32}$ supercell. For each Mn and N concentration we have studied the preferred sites of Mn and N atoms in the supercell by calculating the total energies for various choices of the replacement sites. For clarity of sites chosen, we have numbered all the Zn and O atoms in the $Zn_{32}O_{32}$ supercell (see Fig. 1). For each configuration, the atomic positions in the top two and bottom two layers of the supercell were fully relaxed without any symmetry constraint. The total energies were calculated using the projected augmented wave method as implemented in the *Vienna Ab initio Simulation Package*.[11] The calculations were performed using the generalized gradient approximation in the density functional theory.[12] The *k*-points convergence was achieved with $(6\times4\times1)$ Monkhorst-Pack grid.[13] Tests performed with up to $(8\times6\times2)$ *k*-point mesh indicated that our result based on the smaller grid is quantitatively reliable. The energy cutoff in the plane wave basis was 350 eV. The convergence in energy and threshold for force optimization were set at 10^{-4} eV and 3×10^{-3} eV/Å, respectively. To determine the magnetic coupling between Mn atoms, it is necessary to dope the thin film with at least two Mn atoms, and calculate the total energies by allowing the Mn spins to couple both ferromagnetically and antiferromagnetically.

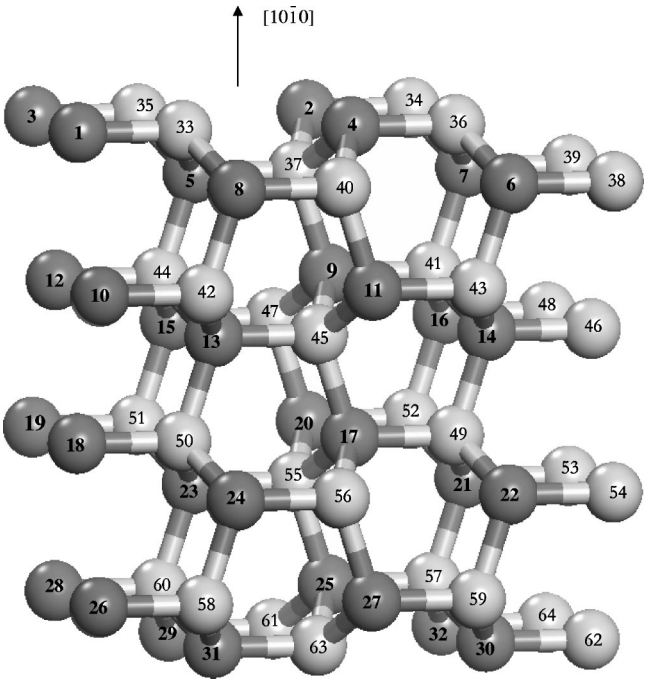

FIG. 1. The side view of ZnO (10$\bar{1}$0) surface. The dark atoms are Zn and lighter atoms are O.

We first summarize our results on ZnO (10$\bar{1}$0) thin film doped with Mn. Details of these results can be found elsewhere.[14] Due to the symmetry of the slab, we chose a $Zn_{28}Mn_4O_{32}$ supercell where two Mn atoms were substituted at two specific Zn sites on the top two layers of the slab, as shown in Fig. 1. The symmetry of the slab then requires that the corresponding Zn sites on the bottom two layers also be replaced by Mn. We chose six different configurations for Mn substitution. These corresponded to replacing Zn sites marked (Nos. 2, 4), (Nos. 2, 3), (Nos. 2, 5), (Nos. 2, 8), (Nos. 5, 8), and (Nos. 5, 6) (defined as configuration I–VI, in sequence), respectively. Note that in these configurations, the Mn-Mn separation, as well as their nearest neighbor environment vary. For each of the earlier configurations, we studied the total energies of the antiferromagnetic (AFM) and ferromagnetic (FM) coupling between Mn spins. We found that the most preferred configuration is the one in which two Mn atoms occupy the nearest neighbor (Nos. 2, 4) sites in the surface layer. The antiferromagnetic state is lower in energy than the ferromagnetic state by 0.133 eV/Mn atom. The O atoms near Mn impurities are polarized ferromagnetically. The next most favorable configuration has Mn atoms in the second layer, again occupying the nearest neighbor (Nos. 5, 8) sites. The antiferromagnetic and ferromagnetic states are 0.041 eV/Mn atom and 0.094 eV/Mn atom above the ground state configuration, respectively. For each of the remaining four configurations, we also found the antiferromagnetic state to be lower in energy than the ferromagnetic state.

We have explored the possibility that the (Zn,Mn)O system when codoped with N could turn into a ferromagnet as N would introduce hole carriers. These in turn could mediate the ferromagnetic coupling between Mn spins. We have studied this possibility by doping with four different concentrations of nitrogen. The corresponding four supercells used are $Zn_{28}Mn_4O_{30}N_2$, $Zn_{28}Mn_4O_{28}N_4$, $Zn_{28}Mn_4O_{26}N_6$, and $Zn_{28}Mn_4O_{24}N_8$, which amount to 6.25%, 12.5%, 18.75%, and 25.0% N substitution at O sites. For each of these concentrations we again studied the energetics of various configurations by replacing different Zn and O sites with Mn and N respectively. In the following we discuss each of these concentrations in sequence.

1. $Zn_{28}Mn_4O_{30}N_2$. Total energies were calculated for both FM and AFM configurations by replacing two Zn sites (Nos. 2, 4) with Mn, and O site (No. 37) with N, as shown in Fig. 1. The corresponding sites on the bottom layers were similarly replaced to preserve symmetry. The calculations were repeated with Mn replacing Zn sites (Nos. 5, 8) and N replacing O at site (No. 33). The ground state configuration is again found to be antiferromagnetic, in which the two Mn atoms form nearest neighbors on the surface with the N atom binding to both the Mn atoms (see Table I and Fig. 1). Unlike the case of $Zn_{28}Mn_4O_{32}$, where the FM state was 0.133 eV/Mn atom above the AFM state, the energy difference between AFM and FM states in the N-doped sample is considerably reduced. The FM state is only 0.045 eV/Mn

TABLE I. Relative energies of antiferromagnetic and ferromagnetic configurations of N-doped (Zn,Mn)O. The first column gives the composition of the supercell, while the second and third columns give the Zn and O sites that were replaced by Mn and N, respectively, (see Fig. 1). The ground state energy is defined as 0.000. The relative energies of the other magnetic states, measured with respect to the ground state energy for each supercell, are given in columns 4 and 5. The last column gives the spin alignments of the Mn atoms and the interlocking O or N atoms (x) for the ground magnetic configuration only ("↑" means spin up and "↓" means spin down).

System	# site occupied by Mn	# site occupied by N	Relative energies (eV/Mn atom) AFM	FM	Mn-x-Mn
$Zn_{28}Mn_4O_{32}$	(2, 4)	···	0.000	0.133	↑-↑-↓
	(5, 8)	···	0.041	0.094	↑-↑-↓
$Zn_{28}Mn_4O_{30}N_2$	(2, 4)	(37)	0.000	0.045	↑-↑-↓
$Zn_{28}Mn_4O_{28}N_4$	(2, 4)	(37, 40)	0.011	0.000	↑-↓-↑
$Zn_{28}Mn_4O_{26}N_6$	(5, 8)	(33, 35, 37)	0.017	0.000	↑-↓-↑
$Zn_{28}Mn_4O_{24}N_8$	(5, 8)	(33, 35, 37, 40)	0.028	0.000	↑-↓-↑

atom above the AFM state. We should recall that in a cluster of Mn_2N, the FM state is lower in energy than the AFM state.[15] This demonstrates the influence of the ZnO matrix on the relative stability of the FM and AFM states. We further note that small concentrations of N cannot cause a transition from AFM to FM state.

2. $Zn_{28}Mn_4O_{28}N_4$. At this nitrogen concentration, we have calculated the total energies corresponding to AFM and FM states for four different configurations. These correspond to replacing Zn sites (Nos. 2, 4) and O sites (Nos. 34, 36); Zn sites (Nos. 2, 4) and O sites (Nos. 37, 40); Zn sites (Nos. 5, 8) and O sites (Nos. 33, 35); and Zn sites (Nos. 5, 8) and O sites (Nos. 37, 40) with Mn and N atoms, respectively. In Table I we present only the ground state configuration. Results for other configurations can be provided upon request. We find the ground state configuration to be FM and 0.011 eV/Mn atom lower in energy than the AFM state. In this configuration the Mn atoms occupy the nearest neighbor surface sites (Nos. 2, 4) with the two N atoms binding to the Mn atoms on sites (Nos. 37, 40). As the N atoms are moved to different sites, e.g., to sites (Nos. 34, 36), the AFM state becomes the more favorable state.

3. $Zn_{28}Mn_4O_{26}N_6$. At this nitrogen concentration, we examined three different configurations for Mn and N substitutions. In the first configuration, we substituted Zn sites (Nos. 2, 4) with Mn and O sites (Nos. 36, 37, 40) with N. In the second configuration, Zn sites (Nos. 5, 8) were replaced by Mn and O sites (Nos. 33, 35, 37) were replaced with N. In the third configuration, we also replaced Zn sites (Nos. 5, 8) with Mn, but replaced O sites (Nos. 35, 37, 40) with N. The second configuration with FM coupling between Mn spins was the ground state and lies 0.017 eV/Mn atom below the AFM state.

4. $Zn_{28}Mn_4O_{24}N_8$. We have studied six different configurations for the substitution of Zn by Mn and O by N atoms. Theses correspond to Zn sites and O sites marked by (Nos. 2, 4; 34, 36, 37, 40), (Nos. 2, 3; 35, 37, 34, 39), (Nos. 2, 5; 33, 35, 37, 34), (Nos. 2, 8; 33, 34, 37, 40), (Nos. 5, 8; 33, 35, 37, 40), and (Nos. 5, 6; 36, 34, 40, 37), These configurations are again defined as configuration I–VI. For all these substitutions, we once again computed the total energies for FM and AFM states. The energy difference between AFM and FM for the above six configurations are plotted in Fig. 2 and compared with corresponding results before N codoping. We found the FM state to be lower in energy for all these configurations with the energy difference ΔE ranging from 0.002 to 0.080 eV/Mn atom. However, in Table I we only give the results for the ground state configuration V. In this configuration, the two Mn atoms form nearest neighbors in the second layer with four N atoms binding to both the Mn atoms. The energy of the AFM state is 0.028 eV/Mn atom higher than the FM state.

Origin of ferromagnetic coupling. We now analyze the electronic structure corresponding to the lowest energy configurations of (Zn,Mn)O and N doped (Zn,Mn)O system to understand why ferromagnetism is preferred with increasing N concentration. For the latter we concentrate on the results corresponding to the $Zn_{28}Mn_4O_{24}N_8$ supercell. This is accomplished through a study of the density of states (DOS), as shown in Fig. 3. We begin with the DOS of pure ZnO [Fig. 3(a)], which is characterized by a gap of about 2 eV. In Fig. 3(b) we plot the total DOS corresponding to the $Zn_{28}Mn_4O_{32}$ supercell. Even though the energy gap narrows considerably, the Fermi energy still lies in a region of vanishing electron density. This is due to the fact that the isovalent Mn^{2+} ion does not introduce any carriers. The states near the Fermi energy are dominated by the Mn 3*d* states. The partial density of states around Mn and O atoms occupying sites (No. 4) and (No. 36) are plotted in Fig. 3(c). Note that neither Mn nor O introduce DOS at the Fermi energy although there is hybridization between Mn 3*d* and O 2*p* states.

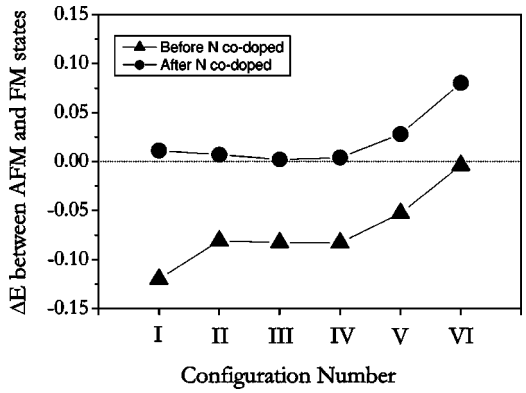

FIG. 2. The energy difference ΔE [$\Delta E = E$(AFM) $- E$(FM) eV/Mn atom] between AFM and FM states for the six configurations which are defined in the text. The solid triangle is for $Zn_{28}Mn_4O_{32}$ the supercell, and the solid circle is for the $Zn_{28}Mn_4O_{24}N_8$ supercell.

In Fig. 3(d) we plot the total DOS corresponding to the $Zn_{28}Mn_4O_{24}N_8$ supercell. Here we see that the Fermi energy passes through the spin-up density states. There are no contributions to the DOS from the spin-down band. The system thus behaves as a half metallic system. To understand the nature of the electrons at the Fermi energy, we have calculated the partial density of states around Mn and N atoms occupying sites (No. 8) and (No. 33) in Fig. 1. These are plotted in Fig. 3(e). We see distinct overlap between Mn 3*d* and N 2*p* states in the spin-up bands which leads to significant DOS at the Fermi energy and hence to the half-metallic character of N codoped (Zn,Mn)O system. In Fig. 3(f) we plot the partial density of states of O 2*p* states occupying site (No. 36) in Fig. 1. Note that O does not contribute electron to the Fermi sea. Thus, it is clear that the ferromagnetism in the $Zn_{28}Mn_4O_{24}N_8$ supercell is caused by hybridization between N 2*p* and Mn 3*d* electrons.

In conclusion, we have shown that by codoping N and Mn, it is possible to make ZnO into a dilute magnetic semiconductor. Mn and N atoms prefer to exist as nearest neighbors in ZnO. The FM state is the result of N 2*p* and Mn 3*d* interaction. Doping N atoms introduces carriers, while doping Mn atoms introduces local magnetic moments. Just as seen in clusters, the magnetic moment of Mn polarizes the spins at the neighboring N sites antiferromagnetically. Ferromagnetism is mediated through the *p-d* exchange interaction between carriers and Mn atoms. It should be pointed out that

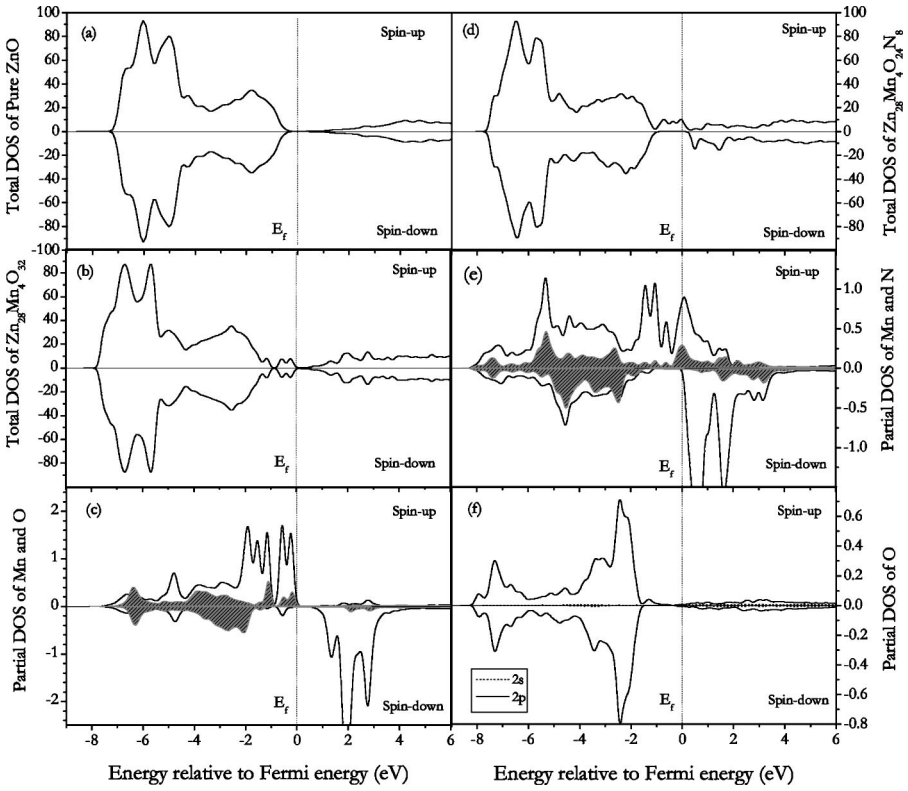

FIG. 3. Total spin DOS of (a) pure $Zn_{32}O_{32}$, (b) Mn doped ZnO ($Zn_{28}Mn_4O_{32}$). (c) Partial spin DOS of Mn 3*d* and O 2*p* (in shade) states in $Zn_{28}Mn_4O_{32}$. (d) Total spin DOS of Mn and N codoped ZnO ($Zn_{28}Mn_4O_{24}N_8$). (e) Partial spin DOS of Mn 3*d* and N 2*p* (in shade) states, and (f) partial spin DOS of O 2*p* state in $Zn_{28}Mn_4O_{24}N_8$.

codoping of ZnO with Mn and N may not be easy. However, some recent experiments provide room for optimism. Matsui and his co-workers,[16] using NO and N_2O source with the radio frequency plasma, were successful in controlling the N concentration systematically. Similarly, Ma and his colleagues[17] have synthesized nitrogen doped ZnO thin films with various nitrogen concentrations by thermal processing of zincoxy nitride alloy films prepared by radio frequency reactive magnetron sputtering. This progress provides some clues for codoping N and Mn in ZnO to realize ferromagnetism in this system. Special experimental techniques may be needed in the practical synthesis. It is hoped that this study will motivate new experimental investigations.

This work was supported in part by a grant from the Office of Naval Research. The authors would like to express their sincere thanks to the crew of the Center for Computational Materials Science, the Institute for Materials Research, Tohoku University, for their continuous support of the HITAC SR8000 supercomputing facility.

*Author to whom correspondence should be addressed.

[1] T. Dietl, H. Ohno, F. Matsukura, J. Cibert, and D. Ferrant, Science **287**, 1019 (2000); H. Ohno, D. Chiba, F. Matsukura, T. Omiya, E. Abe, T. Dietl, Y. Ohno, and K. Ohtani, Nature (London) **408**, 944 (2000).

[2] S. S. Kim, J. H. Moon, B. T. Lee, O. S. Song, and J. H. Je, J. Appl. Phys. **95**, 454 (2004).

[3] M. E. Overberg, C. R. Abernachy, and S. J. Pearton, Appl. Phys. Lett. **79**, 1312 (2001); N. Theodoropoulou and A. F. Hebard, *ibid.* **78**, 3475 (2001); M. L. Reed, N. A. EI-Masary, H. H. Stadelmaier, M. K. Ritums, and M. J. Read, *ibid.* **79**, 3473 (2001).

[4] S. W. Jung, S.-J. An, and G.-C. Yi, Appl. Phys. Lett. **80**, 4561 (2002).

[5] P. Sharma, A. Gupta, K. V. Rao, F. J. Owens, R. Sharma, R. Ahuja, J. M. Osorio Guillen, B. Johansson, and G. A. Gehring, Nat. Mater. **2**, 673 (2003).

[6] T. Fukumura, Z. Jin, M. Kawasaki, T. Shono, T. Hasegawa, S. Koshihara, and H. Koinuma, Appl. Phys. Lett. **78**, 958 (2001).

[7] X. M. Cheng and C. L. Chien, J. Appl. Phys. **93**, 7876 (2003).

[8] Z. Jin, Y.-Z. Yoo, T. Sekiguchi, T. Chikyow, H. Ofuchi, H. Fujioka, M. Oshima, and H. Koinuma, Appl. Phys. Lett. **83**, 39 (2003).

[9] K. V. Rao (private communication).

[10] K. Sato and H. K. Yoshida, Jpn. J. Appl. Phys., Part 2 **40**, L485 (2001); Semicond. Sci. Technol. **17**, 367 (2002).

[11] G. Kresse and J. Furthmuller, Phys. Rev. B **54**, 11 169 (1996).

[12] J. P. Perdew and Y. Wang, Phys. Rev. B **45**, 13 244 (1992).

[13] H. J. Monkhorst and J. D. Pack, Phys. Rev. B **13**, 5188 (1976).

[14] Q. Wang, Q. Sun, B. K. Rao, and P. Jena, Phys. Rev. B **69**, 233310 (2004).

[15] B. K. Rao and P. Jena, Phys. Rev. Lett. **89**, 185504 (2002).

[16] H. Matsui, H. Saeki, T. Kawai, H. Tabata, and B. Mizobuchi, J. Appl. Phys. **95**, 5882 (2004).

[17] J. G. Ma, Y. C. Liu, R. Mu, J. Y. Zhang, Y. M. Lu, D. Z. Shen, and X. W. Fan, J. Vac. Sci. Technol. B **22**, 94 (2004).